Appl. Phys. A 79, 899–901 (2004)
DOI: 10.1007/s00339-004-2801-0

Applied Physics A
Materials Science & Processing

A.H. ROMERO[1]
H.O. JESCHKE[2]
A. RUBIO[3]
M.E. GARCIA[4,5,✉]

Atomistic simulation of the laser induced damage in single wall carbon nanotubes: Diameter and chirality dependence

[1] Advanced Materials Department, IPICyT, Camino a la presa San José 2055, CP 78216, San Luis Potosí, SLP, México
[2] Department of Physics & Astronomy, Rutgers University, 136 Frelinghuysen Road, Piscataway, NJ 08854, USA
[3] Departamento de Física de Materiales, Facultad de Químicas, Universidad del País Vasco, Centro Mixto CSIC-UPV/EHU and Donostia International Physics Center (DIPC), 20018 San Sebastián/Donostia, Spain
[4] Institut für Theoretische Physik, Freie Universität Berlin, Arnimallee 14, 14195 Berlin, Germany
[5] Department de Física, Universitat de les Illes Balears, 07071 Palma de Mallorca, Spain

Received: 1 October 2003/Accepted: 15 March 2004
Published online: 26 July 2004 •

ABSTRACT The effect of high energy laser pulses on single wall carbon nanotubes (SWNT) is studied by a non-equilibrium quantum mechanical model. For the studied laser parameters, we find ablation thresholds that vary between 1.9 eV/atom and 2.3 eV/atom. For zigzag tubes a linear increase of damage thresholds as function of diameter is observed. For armchair tubes, a stability maximum is found at the (10,10) SWNT. We find that below but close to the damage threshold the nanotubes show the presence of standing waves.

PACS 78.70.-g; 52.38.Mf; 61.46.+w

1 Introduction

Short laser pulses are new technology which now is applied to many different materials as probes for following changes in materials at very fast time scales. A very large amount of energy is deposited and the electrons acquire a relatively large temperature which is relaxed to equilibrium by electron-electron or electron-ion interactions on time scales of the order of 1 ps in the case of carbon [1]. Materials which have attracted a lot of attention are carbon nanotubes [2–4]. These sp^2 hybridized structures can theoretically be obtained by rolling a hexagonal graphene sheet in different directions which leads to chiral and non-chiral arrangements [4]. In non-chiral geometries one of the hexagonal bonds is parallel or perpendicular to the tube axis (the parallel case is called a zigzag tube, the perpendicular one is called an armchair tube). Other geometries are chiral and any bond in a hexagon has an angle with respect to the tube axis. Recently, the effects of the irradiation of strong laser fields on metallic and semiconductor carbon nanotubes have been studied [5]. It was concluded that some irreversible changes are present on the tubes which are related to the local increase of temperature. There was some thermal annealing which reordered the carbon tube sample. The authors also noticed a dependence of these morphological changes on tube diameter.

✉ Fax: +49-30/83856799, E-mail: garcia@physik.fu-berlin.de

In this work we address the destroying single pulse laser threshold as function of diameter and chirality of single wall carbon nanotubes. We define the damage threshold as the laser intensity (in eV/atom) necessary to produce an irreversible change in the structure of the nanotube (loss of carbon monomers or permanent tearing of the SWNT walls). For this purpose we have used a theoretical model recently developed by Jeschke et al. [6, 7] to simulate the laser interaction with covalent nanostructures. We see a very strong dependence of the tube behavior on laser parameters, diameter and chirality.

2 Theory

In the investigation of the damage thresholds of carbon nanotubes, we apply a previously developed method [6, 7] of molecular dynamics (MD) simulations on time dependent potential energy surfaces. The MD simulations are based on the Lagrangian [8]

$$L = \sum_{i=1}^{N} \frac{1}{2} m_i \dot{\boldsymbol{s}}_i^t h^t h \dot{\boldsymbol{s}}_i - \frac{1}{2} \sum_{i=1}^{N} \sum_{\substack{j=1 \\ j \neq i}}^{N} \Xi(r_{ij}) + \frac{1}{2} W \mathrm{Tr}(\dot{h}^t \dot{h}) - p_{\mathrm{ex}} \det(h). \quad (1)$$

Here, the absolute coordinates of the atoms $\boldsymbol{r}_i$ are connected via $\boldsymbol{r}_i = h\boldsymbol{s}_i$ to the relative coordinates $\boldsymbol{s}_i$ by the matrix h that contains the vectors spanning the MD supercell. $\Xi(r_{ij})$ is the potential energy that is determined from a tight binding Hamiltonian. The first two terms in the Lagrangian yield the Newton equations of motion for the atoms while the last two terms lead to equations of motion for the additional degrees of freedom for the coordinates of the MD supercell. The external pressure p_{ex} acts on the MD supercell which can change its shape and volume according to its equations of motion. The equations of motion are integrated using the Verlet algorithm [9]. In this study we set the external pressure p_{ex} to 0 in order to permit a free longitudinal expansion of the nanotube upon laser irradiation. This corresponds to the experimental situation that the nanotube is shorter than the diameter of the laser spot (which is usually of the order of tens of μm) and

can freely expand upon laser excitation. Furthermore, experiments on carbon nanotubes are usually conducted under high vacuum conditions. The choice of the parameter W according to the prescription of Andersen [10] ensures that the longitudinal breathing mode of the nanotube occurs at a reasonable frequency.

We derive the interaction potential $\Xi(r_{ij})$ from the tight-binding Hamiltonian in second quantization which we diagonalize at each time step:

$$H_{\mathrm{TB}} = \sum_{i\alpha} \varepsilon_{i\alpha} n_{i\alpha} + \sum_{\substack{ij\alpha\beta \\ j\neq i}} V_{ij}^{\alpha\beta} c_{i\alpha}^{+} c_{j\beta} + \frac{1}{2} \sum_{\substack{ij \\ j\neq i}} \varphi(r_{ij}). \tag{2}$$

Here, the $V_{ij}^{\alpha\beta}$ are hopping integrals with a direction dependence determined according to Slater and Koster [11]. The repulsion of the ionic cores is accounted for by the potential $\varphi(r_{ij})$. For carbon we use tight binding parameters that were developed and tested carefully by Ho et al. [12, 13]. The forces $f_{k\gamma}$ (for atom k, $\gamma = x, y, z$) are determined according to the Hellman–Feynman theorem:

$$f_{k\gamma} = -\sum_{m} \varrho_m \langle m| \frac{\partial H_{TB}(\boldsymbol{r}_1, \ldots, \boldsymbol{r}_N)}{\partial r_{k\gamma}} |m\rangle - \frac{1}{2} \sum_{\substack{ij \\ j\neq i}} \frac{\partial \varphi(r_{ij})}{\partial r_{k\gamma}}. \tag{3}$$

Here, the sum runs over all tight-binding eigenvalues, the occupations of which are given by ϱ_m. $|m\rangle$ are the eigenvectors of the Hamiltonian matrix. We introduce the effect of the ultrashort laser field by solving additional equations of motion for the occupations of the electronic states ϱ_m which thus become explicitly time dependent. Starting from the Liouville–von Neumann equation one finds after some algebra and several approximations

$$\begin{aligned} \frac{\mathrm{d}\varrho(\varepsilon_m, t)}{\mathrm{d}t} = & \int_{-\infty}^{\infty} \mathrm{d}\omega\, g(\omega, t-\Delta t) \Big\{ [\varrho(\varepsilon_m - \hbar\omega, t-\Delta t) \\ & + \varrho(\varepsilon_m + \hbar\omega, t-\Delta t) - 2\varrho(\varepsilon_m, t-\Delta t)] \Big\} \\ & - \frac{\varrho(\varepsilon_m, t) - \varrho^0(\varepsilon_m)}{\tau_1}. \end{aligned} \tag{4}$$

The second term of (4) describes the electron-electron collisions that lead to an equilibration of the electronic system with a rate equation of the Boltzmann type for the distribution $\varrho(\varepsilon_m, t)$. Hence, with a time constant τ_1, the distribution $\varrho(\varepsilon_m, t)$ approaches a Fermi–Dirac distribution $\varrho^0(\varepsilon_m)$.

3 Results

In Fig. 1, we present example snapshots for the laser induced dynamics in a (20,0) zigzag SWNT. The calculation was done for $N = 320$ atoms with periodic boundary conditions at a pressure $p_{\mathrm{ex}} = 0$. In Fig. 1a, the initial tube thermalized to a temperature of $T = 300$ K is shown. The equilibrium structure at room temperature was obtained by performing simulated annealing for 400 fs and subsequently equilibrating the system for 1.6 ps. The obtained average

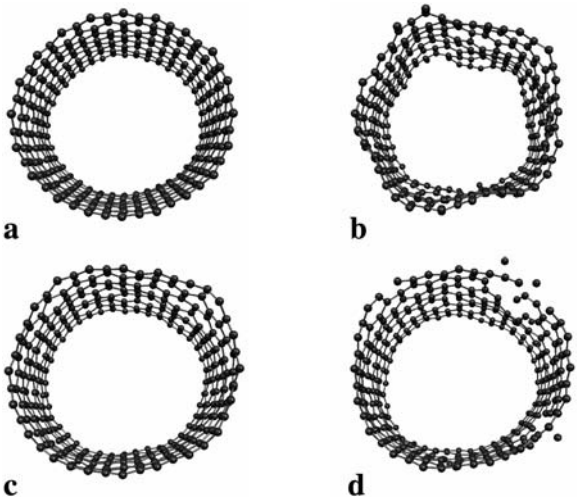

FIGURE 1 Snapshots of our simulations for a (20,0) SWNT at an initial temperature of $T = 300$ K. **a** Initial configuration after thermal relaxation. **b** Configuration after 1 ps simulation after the application of a laser pulse of 2.1 eV/atom, below the laser threshold. Note that a standing wave has formed on the perimeter of the SWNT wall. **c** Configuration at $t = 600$ fs after the action of a pulse of 2.35 eV/atom which is above the damage threshold. Some bonds have been elongated or broken, but no permanent damage has appeared yet. **d** Configuration with the same laser energy as in **c** and after 1 ps. Three carbon monomers are leaving the SWNT

equilibrium diameter of $d = 15.72$ Å is close to the theoretical diameter of $d = 15.65$ Å (with a theoretical C−C distance of 1.42 Å). The laser pulse duration was fixed at 20 fs and the central laser frequency at 1.96 eV. The dependence on these values will be presented in future publications. Figure 1b shows the structure of a tube at a time $t = 1$ ps after the action of a laser pulse of $E_0 = 2.1$ eV/atom. The excitation energy is a little below the damage threshold. Upon action of the laser pulse (here and for all calculations in this paper a pulse duration of $\tau = 20$ fs was used), the nanotube increases its diameter to a maximum value of $d = 17.0$ Å. Subsequently, this vibrational excitation decays into a combination of oscillation modes. One of these modes is the one clearly visible in the figure which corresponds to a time $t = 1$ ps after the pulse maximum. Namely, a standing wave has formed on the wall of the SWNT. In Fig. 1c and d we show two subsequent snapshots of a tube that has absorbed an energy of $E_0 = 2.35$ eV/atom. In Fig. 1c the breathing mode excited by the pulse has led to elongation and breaking of some bonds at time $t = 600$ fs after the peak of the pulse. The maximum amplitude of the breathing mode before bond breaking in this case was $d = 17.2$ Å, and no standing wave was formed on the SWNT wall after the laser excitation. In Fig. 1d three atoms are leaving the SWNT body, indicating that the absorbed energy was above the damage threshold. We have considered relaxation times after the application of the laser pulse varying from 1.0 ps to 2.0 ps depending on the observed situation.

In Fig. 2 we show our results of the damage thresholds of SWNTs as a function of diameter, for pairs of SWNT with similar radius but different chirality. As examples we chose $(n, 0)$ type zigzag tubes and (n, n) type armchair tubes. Furthermore, in Fig. 2 we can discern trends for the damage thresholds of the two types of SWNT as a function of diameter. In the case of the zigzag tubes, the thresholds in-

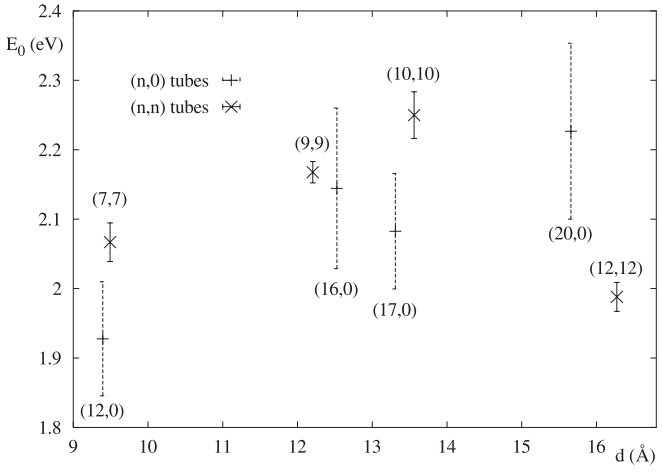

FIGURE 2 Damage thresholds of single wall carbon nanotubes as a function of tube diameter. The duration of the laser pulse was $\tau = 20$ fs. The + *symbols* and *dashed error bars* correspond to tubes of the $(n, 0)$ type, the × *symbols* and *solid error bars* to tubes of (n, n) type

crease with diameter. Meanwhile, the armchair tubes show an increasing damage threshold up to a maximum that occurs for a diameter corresponding to the (10,10) tube. The (12,12) tube shows a significantly lower damage threshold. Our present understanding of the increase of the thresholds with respect to diameter is based on the local strains created by rolling the graphene sheet on the tube. The more narrow the tube, the more the carbon hybridization deviates from the most stable sp^2 configuration and the less energy is needed to break bonds in the SWNT. Close to the threshold we have observed the formation of a standing wave. This is probably a high energy mode which is created only if enough energy is deposited on the tube. From our simulations it seems that if the energy transferred to this mode is high (with respect to its normal amplitude of oscillation) the tube starts to break because the C−C bond becomes larger than allowed. While the general trend in the damage thresholds of Fig. 2 conforms to expectations, we have as yet no explanation for the deviations from this trend, namely the low threshold for the (12,12) tube that makes the more narrow (10,10) tube the most stable of the armchair tubes investigated. A more detailed study will include intermediate diameters in order to clarify if there is indeed a monotonic dependence of the damage thresholds on diameter in the case of the zigzag tubes.

4 Conclusions

We have performed simulations of the interaction of intense laser pulses with single wall carbon nanotubes of different diameters and chiralities. We determined damage thresholds of the nanotubes by analyzing the dynamics of the tubes during 2 ps after the excitation with pulses of $\tau = 20$ fs duration. As an example, we discuss the structural dynamics induced by the laser excitation below and above the damage threshold for the case of a (20,0) SWNT. We find different trends in the damage thresholds as a function of diameter: For the $(n, 0)$ tubes, the thresholds increase with diameter, while they show a maximum at (10,10) for the (n, n) tubes. This study constitutes preliminary results in a more detailed investigation of SWNT stability for many more diameters and laser parameters. It is clear that this study may be important in the case of multiwall nanotubes, where it could be possible to tune the laser to the damage threshold.

ACKNOWLEDGEMENTS AHR acknowledges support from *Millennium Initiative,* Conacyt-Mexico, under Grant W-8001. HOJ gratefully acknowledges support from the DFG through the Emmy Noether Programme. AR was supported by the European Community Research Training Networks NANOPHASE (HPRN-CT-2000-00167) and COMELCAN (HPRN-CT-2000-00128), by Spanish MCyT(MAT2001-0946) and University of the Basque Country (9/UPV 00206.215-13639/2001). M.E.G. acknowledges support from the DFG through SPP 1134 and from the Spanish MCyT through BFM2002-03241 and the Program Ramon y Cajal.

REFERENCES

1 D.H. Reitze, H. Ahn, M.C. Downer: Phys. Rev. B **45**, 2677 (1992)
2 S. Iijima: Nature **354**, 56 (1991)
3 M Terrones: Annu. Rev. Mater. Res. **33**, 419 (2003)
4 M.S. Dresselhaus, G. Dresselhaus, P. Eklund: *The science of fullerenes and carbon nanotubes* (Academic Press, New York 1996)
5 P. Corio, P.S. Santos, M.A. Pimenta, M.S. Dresselhaus: Chem. Phys. Lett. **360**, 557 (2002)
6 H.O. Jeschke, M.E. Garcia, K.H. Bennemann: Phys. Rev. B **60**, R3701 (1999)
7 H.O. Jeschke, M.E. Garcia: *Ultrafast structural changes induced by femtosecond laser pulses*, ed. by B.W. Adams, *Nonlinear Optics, Quantum Optics and Ultrafast Phenomena with X-rays* (Kluwer Academic Publishers, Boston/Dordrecht/London June 2003)
8 M. Parrinello, A. Rahman: J. Appl. Phys **52**, 7182 (1981)
9 L. Verlet: Phys. Rev. **159**, 98 (1967)
10 H.C. Andersen: J. Chem. Phys. **72** 2384 (1980)
11 J.C. Slater, G.F. Koster: Phys. Rev. **94**, 1498 (1954)
12 C.H. Xu, C.Z. Wang, C.T. Chan, K.M. Ho: J. Phys.: Condens. Matter **4**, 6047 (1992)
13 I. Kwon, R. Biswas, C.Z. Wang, K.M. Ho, C.M. Soukoulis: Phys. Rev. B **49**, 7242 (1994)